HHS Public Access

Author manuscript

Basic Res Cardiol. Author manuscript; available in PMC 2018 January 01.

Published in final edited form as:

Basic Res Cardiol. 2017 July ; 112(4): 38. doi:10.1007/s00395-017-0628-z.

Exercise-induced circulating extracellular vesicles protect against cardiac ischemia-reperfusion injury

Yihua Bei[1], **Tianzhao Xu**[1], **Dongchao Lv**[1], **Pujiao Yu**[2], **Jiahong Xu**[2], **Lin Che**[2], **Avash Das**[3], **John Tigges**[4], **Vassilios Toxavidis**[4], **Ionita Ghiran**[4], **Ravi Shah**[3], **Yongqin Li**[1], **Yuhui Zhang**[5], **Saumya Das**[3], and **Junjie Xiao**[1,*]

[1]Cardiac Regeneration and Ageing Lab, School of Life Science, Shanghai University, Shanghai 200444, China

[2]Department of Cardiology, Tongji Hospital, Tongji University School of Medicine, Shanghai 200065, China

[3]Cardiovascular Division of the Massachusetts General Hospital and Harvard Medical School, Boston, MA 02114, USA

[4]Beth Israel Deaconess Medical Center, Boston, and Harvard Medical School, Boston, MA 02215, USA

[5]Heart Failure Care Unit, Fuwai Hospital, State Key Laboratory of Cardiovascular Disease, National Center for Cardiovascular Diseases, Chinese Academy of Medical Sciences and Peking Union Medical College, Beijing 100037, China

Abstract

Extracellular vesicles (EVs) serve an import ant function as mediators of intercellular communication. Exercise is protective for the heart, although the signaling mechanisms that mediate this cardioprotection have not been fully elucidated. Here using a nano-flow cytometry, we found a rapid increase in plasma EVs in human subjects undergoing exercise stress testing. We subsequently identified that serum EVs were increased by ~1.85 fold in mice after 3-week swimming. Intramyocardial injection of equivalent quantities of EVs from exercised mice and non-exercised controls provided similar protective effects against acute ischemia/reperfusion (I/R) injury in mice. However, injection of exercise-induced EVs in a quantity equivalent to the increase seen with exercise (1.85 Swim group) significantly enhanced the protective effect. Similarly, treatment with exercise-induced increased EVs provided additional anti-apoptotic effect in H_2O_2-treated H9C2 cardiomyocytes mediated by the activation of ERK1/2 and HSP27 signaling. Finally, by treating H9C2 cells with insulin-like growth factor-1 (IGF-1) to mimic exercise stimulus *in vitro*, we found an increased release of EVs from cardiomyocytes associated with ALIX and RAB35 activation. Collectively, our results show that exercise-induced increase in circulating EVs enhances the protective effects of endogenous EVs against cardiac I/R injury. Exercise-derived EVs might serve as a potent therapy for myocardial injury in the future.

*Correspondence to: Dr Junjie Xiao, Cardiac Regeneration and Ageing Lab, School of Life Science, Shanghai University, 333 Nan Chen Road, Shanghai 200444, China, Tel: 0086-21-66138131; Fax: 0086-21-66138131; junjiexiao@live.cn.

COMPETING FINANCIAL INTERESTS

The authors declare no competing financial interests.

Keywords

Extracellular vesicles; Exercise; Ischemia-reperfusion injury

INTRODUCTION

Extracellular vesicles (EVs) are a heterogeneous group of lipid encapsulated vesicles (encompassing microvesicles and exosomes) that have captured the attention of scientists for their potential roles in cell-cell communication and cardiovascular biology, disease, and therapeutics [16]. In the past few years, multiple studies have focused on the protective effects of stem cell-derived exogenous EVs against cardiomyocyte apoptosis in the ischemic myocardium [3, 28, 44, 47]. Interestingly, it was recently reported that endogenous plasma EVs could also protect the heart from ischemia-reperfusion (I/R) injury, providing compelling evidence that circulating EVs are able to deliver endogenous protective signals to the heart even in a physiological condition [46].

Exercise training is highly recommended by scientists and clinicians as a key strategy to prevent and treat cardiovascular and metabolic diseases [6]. Exercise is able to trigger the release of a variety of “exerkines” into the circulation that can be contained within EVs [20, 35]. Exercise-derived EVs are hypothesized to be released from cells to the blood and can confer the systemic benefits of exercise to distal organs, including the heart [40]. However current knowledge about the modulation of circulating EVs in response to exercise is limited. One study reported that acute exhaustive exercise can induce rapid release of EVs into the circulation [18]. However, the potential relevance of exercise-derived EVs in cardiovascular biology remains largely unknown. As exercise is widely considered to be protective to the heart, we hypothesized that exercise would further enhance the benefits of endogenous circulating EVs upon ischemic cardiac injury.

In the current study, we investigated the quantity and characteristics of EVs in the plasma of at-risk subjects referred for exercise-testing and found a significant increase in the quantity of EVs (without a marked change in the size) with acute exercise. In parallel, we isolated EVs from the serum of exercised mice and found that circulating EVs were increased by ~1.85 fold in mice after three weeks of swimming exercise when compared with sedentary ones. Interestingly, intramyocardial delivery of equal quantity of EVs isolated from the serum of sedentary mice and exercised mice showed similar protective effects against myocardial I/R injury and cardiomyocyte apoptosis. However, 1.85-fold of exercise-derived EVs further enhanced these cardioprotective effects, indicating that exercise-induced increase in the number, but not change of the contents of circulating EVs was responsible for the additional benefits of exercise. Furthermore, we identified that ERK1/2 and HSP27 activation was essential to mediate the beneficial effects of exercise-derived EVs upon myocardial I/R injury. Finally, we found evidence that exercise-derived EVs may at least in part derive from cardiomyocytes via activation of ALIX and RAB35, though EVs from other sources (e.g. skeletal muscles) deserve further investigation. Taken together, this study demonstrates that exercise is an efficient way to further enhance the protective effects of endogenous circulating EVs to the heart.

METHODS

Exercise testing and plasma collection in human subjects

Patients who were advised exercise stress test for symptomatic or asymptomatic conditions were consented under an approved Institutional Review Board (IRB) Protocol. An intravenous cannulation was performed at rest and three samples of blood, each containing 10 ml were obtained by percutaneous cubital venipuncture drawn in an EDTA containing vacutainer (BD Biosciences, Franklin Lakes, NJ) at three time points (rest, peak exercise, and 15 minutes after the completion of exercise stress test, also termed as recovery). The samples were processed within 60 minutes of blood draw and centrifuged at 1000 x g for 10 minutes in a clinical centrifuge (Eppendorf Centrifuge 5810 R) at room temperature. The plasma from the EDTA tubes were carefully removed leaving the buffy coat aside and transferred to centrifuge tubes (Falcon 15 ml Conical Centrifuge Tubes) and a second spin of 2500 x g for 15 minutes at room temperature was done to pellet any remaining debris. After discarding the lipid-rich topmost layer (500–700 μl) of the plasma, 10 μl was diluted in pre-filtered (through a 0.2 μm filter) phosphate buffered saline (PBS; Life Technologies, Carlsbad, CA) to a final concentration of 1:1000. Plasma diluted in PBS was then transferred in micro-centrifuge tubes (USA Scientific, 1415–2500) that showed no significant ‘shed’ of debris recorded by the instrument in the size range of EVs and indistinguishable from EVs. Similarly, the sheath fluid from the flow cytometer was filtered through a built-in 0.2 μm filter at room temperature. All samples were analyzed by nano-flow cytometry (nano-FCM) within 30 minutes post processing and all procedures were performed at room temperature.

Nano-flow cytometry

Photon Correlation Spectroscopy (PCS) latex beads (100 nm, 200 nm, 300 nm, and 500 nm; PN 6602336, Beckman Coulter, Fullerton, CA), and cell-free plasma were analyzed on the primarily AstriosEQ and also NanoView-equipped MoFlo XDP cell sorter as previously described using a 70 μm nozzle tip with sheath pressure set to 60 PSI [14]. AstriosEQ is equipped with two FSC PMT pathways separated by a beam splitter where FSC1 is a direct laser beam pathway and FSC2 is directed at an angle from the beam splitter. Seven different and unique masks are provided to optimize particle identification and focus laser light to the PMTs, aiding the identification of particles from 200 nm to 30 nm (individually or together). Initial alignment in AstriosEQ was done by acquiring a bead range of 20 μm down to and including 100 nm particles (data not shown). After establishing the dynamic range of the AstriosEQ, the beam splitter was removed and the instrument was optimized on the FSC1 for small particle detection. All subsequent measurements were acquired with threshold set to 561 nm SSC at 0.002–0.005 with no neutral density filter. PCS Mixed Kit was acquired to establish differing size populations and ability to differentiate from noise (signal noise and drop drive noise). All seven masks were processed to establish best mask for nano particle detection. 200 nm polystyrene beads from different manufacturers were compared to show mask sensitivity. Beckman Coulter Flow-Check Pro Flourospheres (cat # A69183) were used to locate beam spot and peak the 488 nm laser and make adjustments to the FSC and SSC-related settings, voltage and threshold (FSC log 425–475V, SSC log 400–450V, FSC or SSC threshold of 0.002%) to optimize the instrument for small particle detection. The threshold parameter used was based on signal to noise ratio of samples being acquired.

Instrument noise was assessed in the absence of any loaded sample by lowering the threshold initially to its minimum of 0.001 and the threshold was then raised to eliminate the events contributed from this noise population. We keep the inherent instrument events (instrument noise) between 800–1500 events per second.

We next proceed by introducing filtered PBS alone, and events generated are visualized. The filtered PBS should not and does not contribute additional events as set forth by defining the background noise (still 800–1500 events per second).

Finally, the experimental samples were measured. We proceed by drawing a gate around the events contributed from the noise population and term it as noise and or background. Within that region of “non EV events”, events are therefore primarily instrument noise, although in the actual samples we cannot exclude that this may contain EVs that are below our instruments limit of detection. A second gate was drawn above the initial gate and was inclusive of all events generated by the experimental sample but excluded noise determined as noted above. This gate was calibrated to latex beads of different sizes (PCS Controls L50, L100, L200, L800, L1000, L1300; cat# 6602784 Beckman Coulter, Inc., 250 S. Kraemer Blvd Brea, CA 92821, U.S.A.) to ensure correct estimation of the **size estimation** of counted EVs. During analysis of all experimental samples, the gates were left the same for consistency and to allow for comparison of the geometric means (GeoMeans). To normalize the **counts** of events in the EV gate of interest, every sample is spiked with 100 μl of 0.5 μm beads at a concentration of 1×10^6/ml and each sample counted for 3 minutes. The number of beads counted for 3 minutes from each sample is consistent across the board and serves as a standard. Percentages reported are normalized based on the bead counts between samples across the board. The EVs were reported through the GeoMeans of the gated populations in the ‘EV’ gate and expressed as percentage of all counted events.

In order to generate a size distribution curve, PCS latex beads (100 nm, 200 nm, and 500 nm) were acquired and adjustments were made to the FSC micrometers and the 488 nm laser micrometers to enhance dynamic range and to optimize signal to noise ratio settings. The beads were mixed for a final bead size distribution curve. To prevent bead aggregation, microbeads were diluted in PBS with 0.1% Tween-20 solution, to a final concentration of 1.29×10^7 beads/mL, and sonicated, and centrifuged at 14,000 x g for 20 minutes to pellet bead aggregates. The topmost 10 μl was further diluted 1:100 before analysis. All controls and samples were acquired at a pressure of 60 PSI and pressure differential of 0.3–0.5 PSI. At this PSI setting and plasma dilution, EVs were processed at 10 k to 20 k events per second. For data analysis of EVs, the mean is chosen due to the scatter properties being logarithmic. The geometric mean (GeoMean) is chosen over the arithmetic mean due to its robustness and not easily being affected by outliers. Therefore, to compare the populations of interest generated on the FSC Log vs SSC Log, the GeoMeans for both axes are compared. The change in GeoMean reflects population shifts and allows for relative size comparisons, while changes in the percentage of events in the EV-gate normalized to bead counts in the 3 minute time-gate allows for estimation of relative EV counts.

Animals and swimming protocol

Eight-week old male C57BL/6 mice were purchased from Cavens Lab Animal (Changzhou, China) and maintained in SPF laboratory animal facility of Shanghai University (Shanghai, China). All animal experiments were conducted under the guidelines on the use and care of laboratory animals for biomedical research published by National Institutes of Health (No. 85–23, revised 1996), and approved by the committee on the Ethics of Animal Experiments of Shanghai University. To induce physiological cardiac growth, a 3-week swimming protocol was performed in mice which could lead to increased heart weight but no alteration in ANP and BNP expressions as our previously reported [34]. In brief, the exercise training began with 5 minutes twice for the first day and 10 minutes twice for the second day, and then continued with an increase of 10 minutes per day until 90 minutes twice per day reached. After 3 weeks of swimming, mice serum was collected for EVs preparation.

Serum EVs preparation

At the end of swimming protocol, 250 μl of mice serum was collected and centrifuged at 3,000 x g for 15 minutes at 4°C. Next, supernatant was incubated with 63 μl of ExoQuick™ Exosome Precipitation Solution (System Biosciences, Mountain View, CA, USA) for 30 minutes and centrifuged at 1500 x g for 30 minutes at 4°C according to the manufacturer's instructions. Supernatant was then removed by aspiration and pelleted fraction was further centrifuged at 1500 x g for 5 minutes at 4°C. Finally, EV pellets were resuspended with 100 μl of PBS and conserved at −80°C for further use.

Transmission electron microscopy and atomic force microscopy

EV pellets were resuspended with 100 μl of PBS, fixed in 2.5% glutaraldehyde for 1 hour, and treated with 1% osmium tetroxide. Section samples at 60 nm were observed under transmission electron microscopy (Jeol JEM-1010, Tokyo, Japan). Additionally, 10 μl of PBS-resuspended EVs were placed onto a mica plate and observed with tapping mode under atomic force microscopy (Agilent 5500 ILM, CA, USA) to visualize the three-dimensional pattern of EVs.

Nanoparticle tracking analysis

EV pellets were resuspended with 100 μl of PBS and subjected to Nanoparticle tracking analysis (NTA) using the NanoSight S300 system (Version 3.1 Build 3.1.54, Malvern, United Kingdom). EVs were captured by the sCMOS Camera at 24.5°C, followed by the measurement of EV particle modal size and concentration.

Intramyocardial injection of EVs and animal model of cardiac ischemia/reperfusion injury

To study the effect of circulating EVs isolated from exercised and sedentary mice, intramyocardial injection of EVs was performed before mice were subjected to cardiac I/R injury. Briefly, equal quantity of EVs (10 μg EVs diluted in 25 μl PBS) isolated from sedentary mice (Baseline group) and exercised mice (Swim group) were injected in the left ventricle free wall before I/R surgery. As the number of circulating EVs was found to be increased by ~1.85 fold after exercise training, intramyocardial injection of 1.85 fold of circulating EVs isolated from exercised mice (1.85 Swim group) was simultaneously

performed to clarify whether exercise-induced increase in the number of EVs could protect and/or produce better effect against I/R injury. Control mice were treated with intramyocardial injection of PBS. After that, mice were subjected to left anterior descending artery (LAD) ligation for 30 minutes, followed by 24 hours of cardiac reperfusion as our previously reported [49]. At 24 hours post I/R injury, 1 ml of 1% Evans Blue dye was injected into the left ventricle. Heart slices were stained with 2,3,5-triphenyltetrazolium chloride (TTC). Infarct size (INF) was measured with staining, whereas the area at risk (AAR) was determined by injecting Evans Blue into the circulation after ligation of the artery, which will be left unstained. The area at risk/left ventricle weight (AAR/LV) ratio was calculated to evaluate the homogeneity of surgery. The infarct area/area at risk (INF/AAR) ratio was calculated to determine the severity of cardiac I/R injury.

Tunel assay for myocardial apoptosis

To evaluate myocardial apoptosis, 5 μm-thick frozen heart sections were fixed in 4% paraformaldehyde (PFA) for 20 minutes, permeabilized with 0.2% Triton X-100 in PBS for 20 minutes, and then blocked with 5% bovine serum album (BSA) for 1 hour at room temperature. To label cardiomyocytes, heart sections were first incubated with mouse anti-α-actinin (Sigma, A7811, 1:200) at 4°C overnight. After incubated with corresponding secondary antibody at room temperature for 2 hours, sections were stained with Tunel FITC Apoptosis Detection Kit (Vazyme, A111-03) according to the manufacturer's instructions. Nuclei were counterstained with DAPI. Finally, 20–30 fields/section were viewed at 400 x magnification under confocal microscope (Carl Zeiss). The percentage of Tunel-positive cardiomyocytes was calculated to determine myocardial apoptosis upon I/R injury.

Cell culture and treatment

Rat H9C2 cardiomyocytes were cultured in Dulbecco's modified eagle's medium (DMEM, Corning, USA) containing 4.5 g/L glucose supplemented with 10% fetal bovine serum (BioInd, Israel) and 1% streptomycin/penicillin at 37°C with 5% CO_2. Treatment of H9C2 cells with hydrogen peroxide (H_2O_2) at 600 μM for 2 hours was used to induce apoptosis. To investigate the potential role of EVs in cardiomyocyte apoptosis, EVs extracted from the serum of sedentary and exercised mice were divided into groups as follows: (1) Baseline group: EVs (10 μg/ml in culture medium) from sedentary mice; (2) Swim group: EVs (10 μg/ml in culture medium) from exercised mice; (3) 1.85 Swim group: 1.85-fold EVs (18.5 μg/ml in culture medium) from exercised mice, compared to (4) Control group: no EVs. Briefly, cells were pre-incubated with serum-derived EVs or control for 24 hours, and H_2O_2 (600 μM) was added 2 hours before the end of incubation. Twenty-four hours after, cells were collected for flow cytometry or Western blot analysis. To clarify whether ERK1/2 and HSP27 activation was essential to mediate the functional role of EVs in the control of cardiomyocyte apoptosis, H_2O_2-treated H9C2 cells were pre-incubated with 1.85 Swim EVs, in the presence of either 50 μM PD98059 (ERK1/2 inhibitor) or 10 μM SB203580 (p38MAPK inhibitor which leads to reduced HSP27 phosphorylation) treatment. To study the potential mechanism how exercise triggers the release of EVs, H9C2 cells were transfected with either ALIX or RAB35 siRNA (75 nM) for 48 hours, and insulin-like growth factor-1 (IGF-1, 100 ng/ml) was added 24 hours before the end of incubation which mimicked exercise stimulus *in vitro*. Finally, the EVs were extracted from the culture

medium using ExoQuick-TC™ Exosome Precipitation Solution (System Biosciences), and exosomal protein concentrations were determined using BCA Protein Assay Kit (TaKaRa).

PKH67 labeling for EVs

To determine whether EVs could be uptaken into H9C2 cells, mouse serum-derived EVs were stained with PKH67 (Sigma, PKH67GL) to allow for particle detection. In brief, 100 μl of PBS-resuspended isolated EVs were dissolved in 1 ml Diluent C containing 4 μl PKH67. After 4 minutes, PKH67 labeling was stopped by adding 2 ml of 0.5% BSA. EVs were then centrifuged at 100,000 g for 1 hour and resuspended in 100 μl of PBS. Next, 10 μg/ml of PKH67-labeled EVs were added into the culture medium of H9C2 cells and incubated for 24 hours. One hour before the end of incubation, Dil dye was added for cell membrane staining. Nuclei were counterstained with DAPI. Images were taken at 600 x magnification under confocal microscope (Carl Zeiss). The presence of PKH67 labeled EVs within H9C2 cells was examined for validation of intake of EVs.

Flow cytometry for cell apoptosis

After cells were pre-treated with serum-derived EVs for 24 hours and stimulated with H_2O_2, cell apoptosis was analyzed using Annexin V-FITC/PI Apoptosis Kit (Bioworld, Nanjing, China) according to the manufacturer's instructions. Briefly, cells were trypsinized and washed twice with PBS. After added with binding buffer and incubated with 2.5 μl of Annexin V-FITC and 2.5 μl of FIPI for 15 minutes in the dark, cells were analyzed for apoptosis and necrosis by flow cytometry (Beckman Coulter, USA).

Western blot analysis

The EV pellets (EV-rich fraction) and supernatants (no-EV fraction) collected from the last step of EV preparation via ExoQuick™ Exosome Precipitation Solution (System Biosciences, Mountain View, CA, USA) were lysed within RIPA lysis buffer (Beyotime, China). The total protein concentration was evaluated by BCA Protein Assay Kit (TaKaRa). Proteins were separated in 10% SDS-PAGE gels and then transferred onto PVDF membranes. After blocked with 5% BSA, the membranes were blotted with rabbit anti-CD63 (System Biosciences, EXOAB-CD63A-1, 1:1000) to confirm the presence and purity of isolated EVs *versus* relative supernatants. For rat H9C2 cardiomyocytes cultured *in vitro* and left ventricle samples from I/R mouse model *in vivo*, cells or tissues were lysed within RIPA lysis buffer (Beyotime, China) complemented with 1% phenylmethylsulfonyl fluoride (PMSF) and Pierce™ protease and phosphatase inhibitor (Thermo, 88668). Equal amount of proteins were subjected to Western blot analysis according to a standard protocol as described above. The membranes were blotted at 4°C overnight with primary antibodies as follows: rabbit-anti-Bax (Abclonal, A0207, 1:1000), rabbit-anti-Bcl2 (Abclonal, A2845, 1:1000), rabbit-anti-pERK1/2 (Abclonal, AP0472, 1:1000), rabbit-anti-total ERK1/2 (Abclonal, A0229, 1:1000), rabbit-anti-pHSP27 (Abcam, ab115891, 1:1000), rabbit-anti-total HSP27 (Abclonal, A0240, 1:1000), rabbit-anti-ALIX (Abclonal, A2215, 1:1000), rabbit-anti-HRS (Abclonal, A1790, 1:1000), rabbit-anti-RAB27B (Abclonal, A10389, 1:1000), rabbit-anti-RAB35 (Abclonal, A8030, 1:1000). The β-actin (Bioworld, BS13278, 1:1000 dilution) was used as a loading control. The blots were then incubated with corresponding secondary antibodies, and finally visualized with enhanced

chemiluminescence (ECL) kit in ChemiDoc XRS Plus luminescent image analyser (Bio-Rad).

Quantitative real-time polymerase chain reactions (qRT-PCRs)

Total RNA was extracted from H9C2 cells using Trizol (TaKaRa) and reverse transcribed using Bio-Rad iScript™ cDNA Synthesis Kit. A template equivalent of 400 ng of total RNA was subjected to 40 cycles of quantitative PCR with Takara SYBR Premix Ex Taq™ (Tli RNaseH Plus, Japan) on CFX96™ Real-Time PCR Detection System (Bio-Rad). 18s was used as an internal control. The primers used were listed in Table 1.

Statistical analysis

All data were analysed using SPSS (version 19.0) and presented as mean ± SEM. A paired-samples t-test was used to compare the circulating EVs in individual patient during resting state and at peak exercise. Apart from this, an independent-sample t-test was used to compare between two groups. For the comparison among (more than) three groups, one-way ANOVA test was performed followed by Bonferroni's post-hoc test. A P value less than 0.05 was settled as the limit of statistical significance.

RESULTS

Circulating EVs are increased acutely with exercise in human subjects

A total of 16 patients were enrolled for the study and peripheral blood samples were collected at baseline (prior to starting exercise) and at peak exercise (right at termination of the protocol). Plasma was processed and analyzed using nano-flow cytometry (nano-FCM) as previously described [14]. The mean age of the patients was 54±11 years and the mean Body Mass Index (BMI) was 27±4 kg/m^2. Among the patients, only 3 were females and 13 had one or more cardiometabolic risk factors (Supplementary Table 1). Analysis of the nano-FCM results demonstrated the presence of a large population of EVs (Fig. 1a) with some variance of sizes at baseline as has been previously reported [14]. We observed a significant increase in the population of EVs in the gate based on forward and side scatter characteristics (normalized to standardized spike-in beads) and previously shown to correspond to EVs during peak exercise in patients compared to their resting state (43.11% ±24.61% *vs* 54.65%±25.68%, $P<0.05$, paired t-test, 2 tailed) (Fig. 1b). This shift in the profile of EVs at peak exercise compared to resting state in patients was noted consistently throughout individual patient samples (Fig. 1c), although there was considerable variation in the baseline levels of EVs as measured by nano-FCM.

Serum EVs are increased by chronic exercise training

We next sought to determine if chronic exercise would lead to a sustained increase in circulating EVs, and whether these exercise-derived circulating EVs have cardioprotective effects. Male adult mice were subjected to a 3-week swimming exercise which was able to induce physiological cardiac growth as previously reported [43], and sedentary mice were used as controls. At the end of three weeks, circulating EVs were extracted from the serum. Using transmission electron microscope and atomic force microscope, we first identified the EVs that were ~100 nm in diameter (Fig. 2a) and 40–50 nm in height (Fig. 2b). Western blot

analysis showed the presence of exosomal marker CD63 in EVs-rich fraction, while the supernatant fraction barely expressed CD63 (Fig. 2c), confirming that EVs were correctly and efficiently extracted from the serum.

Interestingly, based on a nanoparticle tracking analysis, we further detected that the number of circulating EVs isolated from the serum was significantly increased by ~1.85 fold upon exercise training, though the modal size of particles were unchanged (Fig. 2d). Meanwhile, CD63 expression level was also found to be elevated in exercise-derived EVs compared with control ones (Fig. 2e). These data revealed that circulating EVs can be efficiently increased upon chronic exercise.

Exercise-derived circulating EVs reduce myocardial I/R injury *in vivo*

It was previously reported that plasma EVs isolated from healthy human and rats were protective against cardiac I/R injury [46]. However, it is not clear if exercise-derived circulating EVs could produce the same or even more beneficial effects. Here, intramyocardial injections of serum-derived EVs were conducted just before mice were subjected to myocardial I/R injury (30 min ligation and 24 hr reperfusion). As evidenced by TTC staining, the infarct size was markedly reduced by injection with the equal quantity of circulating EVs isolated from sedentary mice (Baseline group) and exercised mice (Swim group) in comparison to that of PBS-injected mice (Fig. 3a), suggesting that exercise-derived EVs (when used in the same quantity as the EVs isolated from sedentary mice) produced the equivalent (but not better) effect against I/R injury.

As we have already identified that the number of circulating EVs isolated from the serum was increased by ~1.85 fold upon exercise training (Fig. 2d), we continued to investigate whether the increase in the number of EVs could account for the cardioprotective effect of exercise against I/R injury. Interestingly, intramyocardial injection with 1.85 fold of EVs isolated from exercised mice (1.85 Swim group) further reduced the infarct size as compared to Swim group (Fig. 3a). As a hallmark of cellular response upon I/R injury, myocardial apoptosis was then evaluated by Tunel staining and Western blot analysis. Our data demonstrated that both of the Baseline group and Swim group had reduced Tunel-positive cardiomyocytes with increased Bcl-2 but reduced Bax expression level in the condition of I/R injury, and 1.85 Swim group showed further enhanced anti-apoptotic effects (Fig. 3b, c). These data indicate that circulating EVs can protect against myocardial I/R injury and apoptosis, and exercise-induced increase of circulating EVs further enhances these effects.

Exercise-derived circulating EVs reduce cardiomyocyte apoptosis *in vitro*

To further clarify the functional effect and molecular mechanism of exercise-derived circulating EVs on cardiomyocyte apoptosis, rat H9C2 cardiomyocytes were pretreated with serum-derived EVs and then exposed to H_2O_2 as an *in vitro* model of apoptosis [49]. As evidenced by PKH67 immunofluorescent labeling, we confirmed that serum-derived EVs could be efficiently taken into H9C2 cardiomyocytes after 24 hours of incubation (Fig. 4a). Moreover, pre-incubation with serum-derived EVs isolated from either sedentary mice (Baseline group) or exercised mice (Swim group) could markedly reduce cellular apoptosis with increased Bcl-2 but reduced Bax expression level, and 1.85 Swim group produced

better anti-apoptotic effect in H_2O_2-treated H9C2 cardiomyocytes (Fig. 4b, c). These results provide direct evidence that serum-derived EV*s* can reduce cardiomyocyte apoptosis *in vitro*, and exercise- induced increase of circulating EVs further enhances this effect.

ERK1/2 and HSP27 can be activated by exercise-derived circulating EVs

The activation of ERK1/2 signaling and subsequent HSP27 phosphorylation has already been well recognized for its cardioprotective effects [46]. Here we found that ERK1/2 and HSP27 phosphorylation levels were increased in H9C2 cardiomyocytes incubated with serum-derived EVs isolated from either sedentary mice (Baseline group) or exercised mice (Swim group), regardless of H_2O_2 treatment (Fig. 5a, b). Meanwhile, ERK1/2 and HSP27 activations were further enhanced in H9C2 cardiomyocytes from the 1.85 Swim group (Fig. 5a, b). As expected, ERK1/2 and HSP27 phosphorylation levels were also found to be elevated in the heart samples from I/R mouse model treated with serum-derived EVs (both Baseline group and Swim group), and to be further enhanced in the 1.85 Swim group (Fig. 5c).

In order to clarify whether ERK1/2 and HSP27 activations are involved in the protective effect of exercise-derived EVs against cardiomyocyte apoptosis, PD98059 (ERK1/2 inhibitor) and SB203580 (p38MAPK inhibitor which leads to reduced HSP27 phosphorylation) were used to treat H9C2 cardiomyocytes. We first confirmed that ERK1/2 and HSP27 phosphorylation could be efficiently reduced by PD98059 and SB203580 *in vitro*, respectively (Fig. 6a, b). Of note, ERK1/2 inhibition via PD98059 led to reduced phosphorylation of HSP27 (Fig. 6c), while HSP27 inhibition via SB203580 did not alter ERK1/2 phosphorylation level (Fig. 6d), confirming that ERK1/2 is an upstream regulator of HSP27 phosphorylation as previously reported [46]. Finally, flow cytometry demonstrated that inhibition of ERK1/2 or HSP27 could totally abolish the anti-apoptotic effect of exercise-derived EVs (1.85 Swim) in H_2O_2-treated cardiomyocytes (Fig. 6e). These data consistently indicate that exercise-induced increase of circulating EVs protects against cardiomyocyte apoptosis via activation of ERK1/2 and HSP27.

IGF-1 induces EVs release from cardiomyocytes via RAB35 and ALIX activation *in vitro*

Though exercise-derived circulating EVs were proved to be protective against myocardial I/R injury and apoptosis, the cellular sources and molecular mechanisms responsible for exercise-derived circulating EVs remain largely unclear. In the present study, we first tried to determine whether the release of EVs could be increased in cultured cardiomyocytes upon treatment with IGF-1, which mimicked the physiological stimulus from exercise. We detected that IGF-1 was sufficient to increase the release of EVs from H9C2 cardiomyocytes into the culture medium (Fig. 7a).

As the release of EVs was increased in IGF-1 treated cardiomyocytes, we continued to examine the genes responsible for EVs formation and secretion. Our results showed that IGF-1 treated H9C2 cells had upregulated HRS, ALIX, RAB27B, and RAB35 at mRNA level (Fig. 7b), while STAM1, TSG101, RAB11, and RAB27A were unchanged (Supplementary Fig. 1). Moreover, ALIX and RAB35 were also found to be upregulated at protein level in both IGF-1 treated H9C2 cells and exercised mice hearts (Fig. 7c, d). To

further elucidate the role of ALIX and RAB35 in the release of EVs, siRNAs targeting ALIX and RAB35 were transfected to H9C2 cells to see if inhibition of these molecules could eliminate IGF-1-induced release of EVs from cardiomyocytes. Our results demonstrated that knockdown of ALIX and RAB35 could significantly reduce the release of EVs from IGF-1 treated H9C2 cells (Fig. 7e), confirming that ALIX and RAB35 activations were necessary to increase the release of EVs from cardiomyocytes upon IGF-1, as a surrogate for exercise *in vitro*.

DISCUSSION

EVs are released from cells and have been shown to carry DNA, mRNA, protein, lipid, as well as a wide range of non-coding RNA, thus serving as important mediators of intercellular communication [39]. EVs and composite cargos have been increasingly shown to contribute to the development of cardiovascular diseases [12]. Therapeutic delivery of exogenous EVs, especially stem cell-derived EVs, have been proposed as a cell-free approach to provide cardioprotective factors to ameliorate cardiomyocyte apoptosis and cardiac ischemic injury [4]. Interestingly, endogenous plasma EVs isolated from healthy humans and rats were also demonstrated to mediate cardioprotection in I/R injury [46]. As exercise can trigger the release of EVs into the circulation, thereby providing a possible mechanism for the systemic benefits of exercise [40], the present study focused on whether physiological exercise-derived endogenous EVs could further enhance the cardioprotective effects of EVs. Intriguingly, we found that circulating EVs were increased in response to an acute bout of exercise in human subjects with cardiometabolic risk, and this increase was persistent in a murine model of endurance exercise. This increase in circulating EVs was correlated with enhanced protective effect against I/R injury *in vivo* and cardiomyocyte apoptosis *in vitro* via activation of ERK1/2 and HSP27 signaling.

Despite the great advances that have been achieved in basic and clinical research for cardiac I/R injury, it still lacks effective interventions in man [7, 8, 22, 24]. The protective effects of exercise against cardiac I/R injury have been well acknowledged [19, 31, 38, 50], which could be associated with reduced myocardial inflammation, minimized oxidative and nitric-oxidative stress, decreased cardiomyocyte apoptosis, and promoted angiogenesis. It was recently reported that exercise is able to enhance cardiomyocyte renewal [34, 42], which is necessary to mediate the protective effect of exercise against I/R injury [5]. Moreover, exercise is efficient to reduce cardiac I/R injury both at baseline and in obese diabetic condition, though different molecular mechanisms might be involved [9, 29]. It was previously reported that acute exercise (cycling) could trigger rapid release of EVs into the circulation that might be responsible for mediating its systemic beneficial effects also including the heart [18]. We now have demonstrated that acute running exercise in patients with cardiac risk factors also increased the quantity of plasma EVs (but not the relative size distribution). However, the physiological relevance of exercise-derived EVs was largely unknown [18]. Based on the nanopartical tracking analysis, we found that serum EVs were increased by ~1.85 fold in mice after a 3-week swimming exercise. Interestingly, intramyocardial delivery of exercise-derived EVs and baseline EVs provided similar protective effects against the murine I/R injury *in vivo*. However, exercise-induced increase of EVs (by 1.85 fold) further enhanced the protective effect. Based on H_2O_2-induced

cardiomyocyte apoptosis *in vitro* model, we found that serum EVs isolated from sedentary and swum mice had similar anti-apoptotic effect, and this effect was further enhanced by exercise-induced increase of EVs. Thus, our *in vivo* and *in vitro* evidence consistently suggests that endogenous circulating EVs protect against myocardial I/R injury and apoptosis, and the exercise-induced increase of EVs further enhances these effects.

The activation of ERK1/2 signaling pathway is known to confer cardioprotection [23]. The phosphorylation of ERK1/2 after myocardial I/R injury is thought to be a compensatory beneficial effect in preventing cardiomyocyte apoptosis [26, 27], likely by inactivation of the caspase cascade [10, 45] and inhibition of conformational change in Bax [48]. Interestingly, it was previously demonstrated that plasma EVs could protect against myocardial I/R injury through an activation of ERK1/2 and subsequent phosphorylation of HSP27 [46]. In the present study, we first identified that the ERK1/2 and HSP27 signaling was activated by serum EVs isolated from both sedentary and swum mice in the I/R heart samples or H_2O_2-treated H9C2 cells. We then found that exercise-induced increase of EVs could further enhance ERK1/2 and HSP27 phosphorylation levels. Finally, inhibition of ERK1/2 or HSP27 could totally abolish the anti-apoptotic effect of exercise-induced increase of EVs in H_2O_2-treated H9C2 cells, indicating that the activation of ERK1/2 and HSP27 signaling is a pivotal mechanism mediating the beneficial effect of exercise-derived EVs in preventing cardiomyocyte apoptosis.

Evidence reporting the response of circulating EVs upon exercise is limited [18], and the cellular source as well as the mechanisms responsible for exercise-induced EVs are much less understood. Additionally, the exact identity of the types of EVs released (microvesicles or exosomes) has not been clearly determined, as there is no consensus for precise markers of EV subtypes. Notably, the size distribution does not change significantly with exercise, although the quantity of EVs increases. The technique of nano-FCM used here to profile the EVs in the human subjects allows for rapid and accurate sizing as well as counts of EVs within a gate calibrated by different size beads (and correlates well with atomic force microscopy-based sizing of EVs). Nonetheless, there are caveats with this technique including events that are counted in non-EV gates that may correspond to protein aggregates, hemoglobin or membrane fragments; we have attempted to normalize the events in the EV-gate across samples using time-gated counts of spike-in beads. Nano-FCM cannot yet be used for sorting of EVs for further downstream analysis (such as functional assays as was done for the murine experiments) as the yield of the sorted EVs from mice plasma remains low. Hence we had to use Exoquick reagent (which may not precipitate a pure population of EVs, but does lead to higher yields) for the murine experiments.

One study has previously demonstrated a robust release of EVs into the cardiac extracellular space and vessel lumen after mice were subjected to endurance exercise [11]. Here, based on H9C2 cells stimulated by IGF-1 which activates the same signaling pathway as the physiological stress of exercise *in vivo*, we found an increased release of EVs from cardiomyocytes into the culture medium. Among the EVs biogenesis- and secretion-related genes [13, 30, 37], ALIX and RAB35 were found to be up-regulated in IGF-1-treated H9C2 cells. Moreover, knockdown of ALIX and RAB35 could attenuate IGF-1-induced EVs release from H9C2 cells, indicating that ALIX and RAB35 activation may be important for

exercise-induced increase of EVs. However, in addition to cardiomyocytes, other types of cells could also be important sources for exercise-induced EVs [40]. Skeletal muscle has been proposed to contribute to the release of “exerkines” encapsulated in EVs [2, 17] in response to exercise. In this regard, exercise-induced EVs derived from skeletal muscle deserve further investigation [1, 21, 40].

Our findings that exercise-induced increase of EVs further enhances the protective effects of endogenous circulating EVs against cardiac I/R injury are novel. Actually, in addition to the increase in EVs, the contents of EVs may also change in response to exercise [11, 32, 41]. However, in our *in vivo* and *in vitro* experiments, we were unable to find an improved protection from exercise-derived EVs (Swim group) compared to baseline EVs (Baseline group). Several factors might be taken into consideration. First, although exercise may change EV cargos, this may not be sufficient to provide additional protection in the *in vivo* I/R injury and *in vitro* cardiomyocyte apoptosis models tested in the present study. Second, the protection from exercise-derived EVs due to the change of EV cargos may also be dependent on the mode of exercise [15, 18, 33]. Thus, different types of exercise would need to be tested and the potential of exercise-derived EVs deserve further investigation in other types of cardiac injury. In these cases, it will be of great interest to perform RNA sequencing, proteomics, and metabolomics to reveal the EV cargo profiles in response to exercise [25, 36].

In conclusion, the present study shows that exercise-induced increase of circulating EVs, via activating the ERK1/2 and HSP27 signaling, provides enhanced protection against cardiac I/R injury compared to endogenous EVs at baseline. Exercise-derived EVs might serve as a potent therapy for myocardial injury in the future.

Supplementary Material

Refer to Web version on PubMed Central for supplementary material.

Acknowledgments

This work was supported by the grants from National Natural Science Foundation of China (81570362 and 91639101 to JJ Xiao and 81400647 to Y Bei), the development fund for Shanghai talents (to JJ Xiao), and the National Institutes of Health (NCATS grant UH3 TR000901 to S Das and U01 HL126497 to IG).

References

1. Aoi W, Ichikawa H, Mune K, Tanimura Y, Mizushima K, Naito Y, Yoshikawa T. Muscle-enriched microRNA miR-486 decreases in circulation in response to exercise in young men. Front Physiol. 2013; 4:80.doi: 10.3389/fphys.2013.00080 [PubMed: 23596423]
2. Aoi W, Sakuma K. Does regulation of skeletal muscle function involve circulating microRNAs? Front Physiol. 2014; 5:39.doi: 10.3389/fphys.2014.00039 [PubMed: 24596559]
3. Barile L, Lionetti V, Cervio E, Matteucci M, Gherghiceanu M, Popescu LM, Torre T, Siclari F, Moccetti T, Vassalli G. Extracellular vesicles from human cardiac progenitor cells inhibit cardiomyocyte apoptosis and improve cardiac function after myocardial infarction. Cardiovasc Res. 2014; 103:530–541. DOI: 10.1093/cvr/cvu167 [PubMed: 25016614]
4. Barile L, Moccetti T, Marban E, Vassalli G. Roles of exosomes in cardioprotection. Eur Heart J. 2016; doi: 10.1093/eurheartj/ehw304

5. Bei Y, Fu S, Chen X, Chen M, Zhou Q, Yu P, Yao J, Wang H, Che L, Xu J, Xiao J. Cardiac cell proliferation is not necessary for exercise-induced cardiac growth but required for its protection against ischaemia/reperfusion injury. J Cell Mol Med. 2017; doi: 10.1111/jcmm.13078
6. Bei Y, Zhou Q, Sun Q, Xiao J. Exercise as a platform for pharmacotherapy development in cardiac diseases. Curr Pharm Des. 2015; 21:4409–4416. [PubMed: 26234794]
7. Bell RM, Botker HE, Carr RD, Davidson SM, Downey JM, Dutka DP, Heusch G, Ibanez B, Macallister R, Stoppe C, Ovize M, Redington A, Walker JM, Yellon DM. 9th Hatter Biannual Meeting: position document on ischaemia/reperfusion injury, conditioning and the ten commandments of cardioprotection. Basic Res Cardiol. 2016; 111:41.doi: 10.1007/s00395-016-0558-1 [PubMed: 27164905]
8. Cabrera-Fuentes HA, Aragones J, Bernhagen J, Boening A, Boisvert WA, Botker HE, Bulluck H, Cook S, Di Lisa F, Engel FB, Engelmann B, Ferrazzi F, Ferdinandy P, Fong A, Fleming I, Gnaiger E, Hernandez-Resendiz S, Kalkhoran SB, Kim MH, Lecour S, Liehn EA, Marber MS, Mayr M, Miura T, Ong SB, Peter K, Sedding D, Singh MK, Suleiman MS, Schnittler HJ, Schulz R, Shim W, Tello D, Vogel CW, Walker M, Li QO, Yellon DM, Hausenloy DJ, Preissner KT. From basic mechanisms to clinical applications in heart protection, new players in cardiovascular diseases and cardiac theranostics: meeting report from the third international symposium on “New frontiers in cardiovascular research”. Basic Res Cardiol. 2016; 111:69.doi: 10.1007/s00395-016-0586-x [PubMed: 27743118]
9. Calvert JW, Condit ME, Aragon JP, Nicholson CK, Moody BF, Hood RL, Sindler AL, Gundewar S, Seals DR, Barouch LA, Lefer DJ. Exercise protects against myocardial ischemia-reperfusion injury via stimulation of beta(3)-adrenergic receptors and increased nitric oxide signaling: role of nitrite and nitrosothiols. Circ Res. 2011; 108:1448–1458. DOI: 10.1161/CIRCRESAHA.111.241117 [PubMed: 21527738]
10. Cardone MH, Roy N, Stennicke HR, Salvesen GS, Franke TF, Stanbridge E, Frisch S, Reed JC. Regulation of cell death protease caspase-9 by phosphorylation. Science. 1998; 282:1318–1321. [PubMed: 9812896]
11. Chaturvedi P, Kalani A, Medina I, Familtseva A, Tyagi SC. Cardiosome mediated regulation of MMP9 in diabetic heart: role of mir29b and mir455 in exercise. J Cell Mol Med. 2015; 19:2153–2161. DOI: 10.1111/jcmm.12589 [PubMed: 25824442]
12. Chistiakov DA, Orekhov AN, Bobryshev YV. Cardiac Extracellular Vesicles in Normal and Infarcted Heart. Int J Mol Sci. 2016; :17.doi: 10.3390/ijms17010063
13. Colombo M, Raposo G, Thery C. Biogenesis, secretion, and intercellular interactions of exosomes and other extracellular vesicles. Annu Rev Cell Dev Biol. 2014; 30:255–289. DOI: 10.1146/annurev-cellbio-101512-122326 [PubMed: 25288114]
14. Danielson KM, Estanislau J, Tigges J, Toxavidis V, Camacho V, Felton EJ, Khoory J, Kreimer S, Ivanov AR, Mantel PY, Jones J, Akuthota P, Das S, Ghiran I. Diurnal Variations of Circulating Extracellular Vesicles Measured by Nano Flow Cytometry. PLoS One. 2016; 11:e0144678.doi: 10.1371/journal.pone.0144678 [PubMed: 26745887]
15. Earnest CP, Lupo M, Thibodaux J, Hollier C, Butitta B, Lejeune E, Johannsen NM, Gibala MJ, Church TS. Interval training in men at risk for insulin resistance. Int J Sports Med. 2013; 34:355–363. DOI: 10.1055/s-0032-1311594 [PubMed: 23180210]
16. Emanueli C, Shearn AI, Angelini GD, Sahoo S. Exosomes and exosomal miRNAs in cardiovascular protection and repair. Vascul Pharmacol. 2015; 71:24–30. DOI: 10.1016/j.vph.2015.02.008 [PubMed: 25869502]
17. Forterre A, Jalabert A, Berger E, Baudet M, Chikh K, Errazuriz E, De Larichaudy J, Chanon S, Weiss-Gayet M, Hesse AM, Record M, Geloen A, Lefai E, Vidal H, Coute Y, Rome S. Proteomic analysis of C2C12 myoblast and myotube exosome-like vesicles: a new paradigm for myoblast-myotube cross talk? PLoS One. 2014; 9:e84153.doi: 10.1371/journal.pone.0084153 [PubMed: 24392111]
18. Fruhbeis C, Helmig S, Tug S, Simon P, Kramer-Albers EM. Physical exercise induces rapid release of small extracellular vesicles into the circulation. J Extracell Vesicles. 2015; 4:28239.doi: 10.3402/jev.v4.28239 [PubMed: 26142461]

19. Gomes EC, Silva AN, de Oliveira MR. Oxidants, antioxidants, and the beneficial roles of exercise-induced production of reactive species. Oxid Med Cell Longev. 2012; 2012:756132.doi: 10.1155/2012/756132 [PubMed: 22701757]
20. Gorgens SW, Eckardt K, Jensen J, Drevon CA, Eckel J. Exercise and Regulation of Adipokine and Myokine Production. Prog Mol Biol Transl Sci. 2015; 135:313–336. DOI: 10.1016/bs.pmbts.2015.07.002 [PubMed: 26477920]
21. Guescini M, Canonico B, Lucertini F, Maggio S, Annibalini G, Barbieri E, Luchetti F, Papa S, Stocchi V. Muscle Releases Alpha-Sarcoglycan Positive Extracellular Vesicles Carrying miRNAs in the Bloodstream. PLoS One. 2015; 10:e0125094.doi: 10.1371/journal.pone.0125094 [PubMed: 25955720]
22. Hausenloy DJ, Barrabes JA, Botker HE, Davidson SM, Di Lisa F, Downey J, Engstrom T, Ferdinandy P, Carbrera-Fuentes HA, Heusch G, Ibanez B, Iliodromitis EK, Inserte J, Jennings R, Kalia N, Kharbanda R, Lecour S, Marber M, Miura T, Ovize M, Perez-Pinzon MA, Piper HM, Przyklenk K, Schmidt MR, Redington A, Ruiz-Meana M, Vilahur G, Vinten-Johansen J, Yellon DM, Garcia-Dorado D. Ischaemic conditioning and targeting reperfusion injury: a 30 year voyage of discovery. Basic Res Cardiol. 2016; 111:70.doi: 10.1007/s00395-016-0588-8 [PubMed: 27766474]
23. Hausenloy DJ, Yellon DM. New directions for protecting the heart against ischaemia-reperfusion injury: targeting the Reperfusion Injury Salvage Kinase (RISK)-pathway. Cardiovasc Res. 2004; 61:448–460. DOI: 10.1016/j.cardiores.2003.09.024 [PubMed: 14962476]
24. Heusch G. Molecular basis of cardioprotection: signal transduction in ischemic pre-, post-, and remote conditioning. Circ Res. 2015; 116:674–699. DOI: 10.1161/CIRCRESAHA.116.305348 [PubMed: 25677517]
25. JanssenDuijghuijsen LM, Keijer J, Mensink M, Lenaerts K, Ridder L, Nierkens S, Kartaram SW, Verschuren MC, Pieters RH, Bas R, Witkamp RF, Wichers HJ, van Norren K. Adaptation of exercise-induced stress in well-trained healthy young men. Exp Physiol. 2017; 102:86–99. DOI: 10.1113/EP086025 [PubMed: 27808433]
26. Jeong JJ, Ha YM, Jin YC, Lee EJ, Kim JS, Kim HJ, Seo HG, Lee JH, Kang SS, Kim YS, Chang KC. Rutin from Lonicera japonica inhibits myocardial ischemia/reperfusion-induced apoptosis in vivo and protects H9c2 cells against hydrogen peroxide-mediated injury via ERK1/2 and PI3K/Akt signals in vitro. Food Chem Toxicol. 2009; 47:1569–1576. DOI: 10.1016/j.fct.2009.03.044 [PubMed: 19362115]
27. Jiang X, Guo CX, Zeng XJ, Li HH, Chen BX, Du FH. A soluble receptor for advanced glycation end-products inhibits myocardial apoptosis induced by ischemia/reperfusion via the JAK2/STAT3 pathway. Apoptosis. 2015; 20:1033–1047. DOI: 10.1007/s10495-015-1130-4 [PubMed: 25894538]
28. Khan M, Nickoloff E, Abramova T, Johnson J, Verma SK, Krishnamurthy P, Mackie AR, Vaughan E, Garikipati VN, Benedict C, Ramirez V, Lambers E, Ito A, Gao E, Misener S, Luongo T, Elrod J, Qin G, Houser SR, Koch WJ, Kishore R. Embryonic stem cell-derived exosomes promote endogenous repair mechanisms and enhance cardiac function following myocardial infarction. Circ Res. 2015; 117:52–64. DOI: 10.1161/CIRCRESAHA.117.305990 [PubMed: 25904597]
29. Kleindienst A, Battault S, Belaidi E, Tanguy S, Rosselin M, Boulghobra D, Meyer G, Gayrard S, Walther G, Geny B, Durand G, Cazorla O, Reboul C. Exercise does not activate the beta3 adrenergic receptor-eNOS pathway, but reduces inducible NOS expression to protect the heart of obese diabetic mice. Basic Res Cardiol. 2016; 111:40.doi: 10.1007/s00395-016-0559-0 [PubMed: 27164904]
30. Kowal J, Tkach M, Thery C. Biogenesis and secretion of exosomes. Curr Opin Cell Biol. 2014; 29:116–125. DOI: 10.1016/j.ceb.2014.05.004 [PubMed: 24959705]
31. Li J, Zhang H, Zhang C. Role of inflammation in the regulation of coronary blood flow in ischemia and reperfusion: mechanisms and therapeutic implications. J Mol Cell Cardiol. 2012; 52:865–872. DOI: 10.1016/j.yjmcc.2011.08.027 [PubMed: 21924274]
32. Little JP, Safdar A, Benton CR, Wright DC. Skeletal muscle and beyond: the role of exercise as a mediator of systemic mitochondrial biogenesis. Appl Physiol Nutr Metab. 2011; 36:598–607. DOI: 10.1139/h11-076 [PubMed: 21888528]

33. Little JP, Safdar A, Bishop D, Tarnopolsky MA, Gibala MJ. An acute bout of high-intensity interval training increases the nuclear abundance of PGC-1alpha and activates mitochondrial biogenesis in human skeletal muscle. Am J Physiol Regul Integr Comp Physiol. 2011; 300:R1303–1310. DOI: 10.1152/ajpregu.00538.2010 [PubMed: 21451146]
34. Liu X, Xiao J, Zhu H, Wei X, Platt C, Damilano F, Xiao C, Bezzerides V, Bostrom P, Che L, Zhang C, Spiegelman BM, Rosenzweig A. miR-222 is necessary for exercise-induced cardiac growth and protects against pathological cardiac remodeling. Cell Metab. 2015; 21:584–595. DOI: 10.1016/j.cmet.2015.02.014 [PubMed: 25863248]
35. Lombardi G, Sanchis-Gomar F, Perego S, Sansoni V, Banfi G. Implications of exercise-induced adipo-myokines in bone metabolism. Endocrine. 2016; 54:284–305. DOI: 10.1007/s12020-015-0834-0 [PubMed: 26718191]
36. Malik ZA, Kott KS, Poe AJ, Kuo T, Chen L, Ferrara KW, Knowlton AA. Cardiac myocyte exosomes: stability, HSP60, and proteomics. Am J Physiol Heart Circ Physiol. 2013; 304:H954–965. DOI: 10.1152/ajpheart.00835.2012 [PubMed: 23376832]
37. Ostrowski M, Carmo NB, Krumeich S, Fanget I, Raposo G, Savina A, Moita CF, Schauer K, Hume AN, Freitas RP, Goud B, Benaroch P, Hacohen N, Fukuda M, Desnos C, Seabra MC, Darchen F, Amigorena S, Moita LF, Thery C. Rab27a and Rab27b control different steps of the exosome secretion pathway. Nat Cell Biol. 2010; 12:19–30. sup pp 11–13. DOI: 10.1038/ncb2000 [PubMed: 19966785]
38. Otani H. The role of nitric oxide in myocardial repair and remodeling. Antioxid Redox Signal. 2009; 11:1913–1928. DOI: 10.1089/ARS.2009.2453 [PubMed: 19203224]
39. SELA, Mager I, Breakefield XO, Wood MJ. Extracellular vesicles: biology and emerging therapeutic opportunities. Nat Rev Drug Discov. 2013; 12:347–357. DOI: 10.1038/nrd3978 [PubMed: 23584393]
40. Safdar A, Saleem A, Tarnopolsky MA. The potential of endurance exercise-derived exosomes to treat metabolic diseases. Nat Rev Endocrinol. 2016; 12:504–517. DOI: 10.1038/nrendo.2016.76 [PubMed: 27230949]
41. Seldin MM, Peterson JM, Byerly MS, Wei Z, Wong GW. Myonectin (CTRP15), a novel myokine that links skeletal muscle to systemic lipid homeostasis. J Biol Chem. 2012; 287:11968–11980. DOI: 10.1074/jbc.M111.336834 [PubMed: 22351773]
42. Shi J, Bei Y, Kong X, Liu X, Lei Z, Xu T, Wang H, Xuan Q, Chen P, Xu J, Che L, Liu H, Zhong J, Sluijter JP, Li X, Rosenzweig A, Xiao J. miR-17-3p Contributes to Exercise-Induced Cardiac Growth and Protects against Myocardial Ischemia-Reperfusion Injury. Theranostics. 2017; 7:664–676. DOI: 10.7150/thno.15162 [PubMed: 28255358]
43. Tao L, Bei Y, Lin S, Zhang H, Zhou Y, Jiang J, Chen P, Shen S, Xiao J, Li X. Exercise Training Protects Against Acute Myocardial Infarction via Improving Myocardial Energy Metabolism and Mitochondrial Biogenesis. Cell Physiol Biochem. 2015; 37:162–175. DOI: 10.1159/000430342 [PubMed: 26303678]
44. Teng X, Chen L, Chen W, Yang J, Yang Z, Shen Z. Mesenchymal Stem Cell-Derived Exosomes Improve the Microenvironment of Infarcted Myocardium Contributing to Angiogenesis and Anti-Inflammation. Cell Physiol Biochem. 2015; 37:2415–2424. DOI: 10.1159/000438594 [PubMed: 26646808]
45. Terada K, Kaziro Y, Satoh T. Analysis of Ras-dependent signals that prevent caspase-3 activation and apoptosis induced by cytokine deprivation in hematopoietic cells. Biochem Biophys Res Commun. 2000; 267:449–455. DOI: 10.1006/bbrc.1999.1955 [PubMed: 10623640]
46. Vicencio JM, Yellon DM, Sivaraman V, Das D, Boi-Doku C, Arjun S, Zheng Y, Riquelme JA, Kearney J, Sharma V, Multhoff G, Hall AR, Davidson SM. Plasma exosomes protect the myocardium from ischemia-reperfusion injury. J Am Coll Cardiol. 2015; 65:1525–1536. DOI: 10.1016/j.jacc.2015.02.026 [PubMed: 25881934]
47. Wang Y, Zhang L, Li Y, Chen L, Wang X, Guo W, Zhang X, Qin G, He SH, Zimmerman A, Liu Y, Kim IM, Weintraub NL, Tang Y. Exosomes/microvesicles from induced pluripotent stem cells deliver cardioprotective miRNAs and prevent cardiomyocyte apoptosis in the ischemic myocardium. Int J Cardiol. 2015; 192:61–69. DOI: 10.1016/j.ijcard.2015.05.020 [PubMed: 26000464]

48. Weston CR, Balmanno K, Chalmers C, Hadfield K, Molton SA, Ley R, Wagner EF, Cook SJ. Activation of ERK1/2 by deltaRaf-1:ER* represses Bim expression independently of the JNK or PI3K pathways. Oncogene. 2003; 22:1281–1293. DOI: 10.1038/sj.onc.1206261 [PubMed: 12618753]

49. Xu J, Tang Y, Bei Y, Ding S, Che L, Yao J, Wang H, Lv D, Xiao J. miR-19b attenuates H2O2-induced apoptosis in rat H9C2 cardiomyocytes via targeting PTEN. Oncotarget. 2016; 7:10870–10878. DOI: 10.18632/oncotarget.7678 [PubMed: 26918829]

50. Zhang KR, Liu HT, Zhang HF, Zhang QJ, Li QX, Yu QJ, Guo WY, Wang HC, Gao F. Long-term aerobic exercise protects the heart against ischemia/reperfusion injury via PI3 kinase-dependent and Akt-mediated mechanism. Apoptosis. 2007; 12:1579–1588. DOI: 10.1007/s10495-007-0090-8 [PubMed: 17505785]

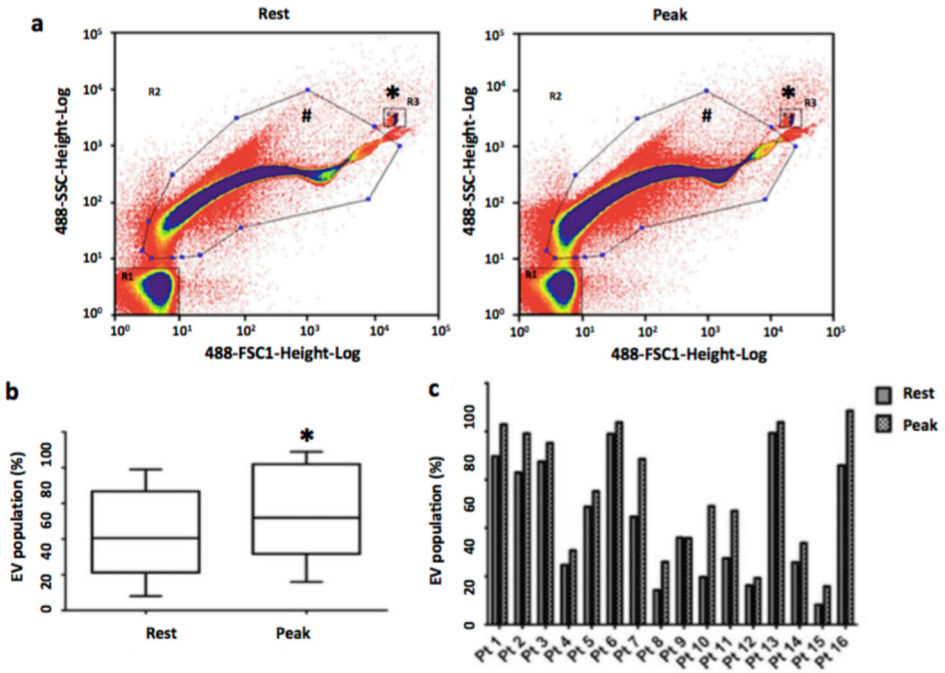

Figure 1. Acute exercise increases extracellular vesicle numbers in human subjects with cardiometabolic risk factors

(a) Nano-FCM demonstrating EV profiles in patients in response to exercise during Exercise Stress Test. Representative nano-FCM profiles were shown at baseline (left) and at peak exercise (right). The rectangular gating (denoted by *) at the right upper quadrant denotes the fluorescent beads sized at 200 nm. EVs are in the gating denoted by hash symbol **(b)** Box-and-whisker plot demonstrating EV population (reported through the GeoMeans of the gated populations and expressed as percentage of the EV-gated population to all counted events) pooled from all the patient samples. **(c)** Bar graph demonstrating EV population (reported through the GeoMeans of the gated populations and expressed as percentage of the EV-gated population to all counted events) in individual patient (Pt) during resting state and at peak exercise. EVs, extracellular vesicles. *, $P<0.05$ (paired t-test, 2 tailed).

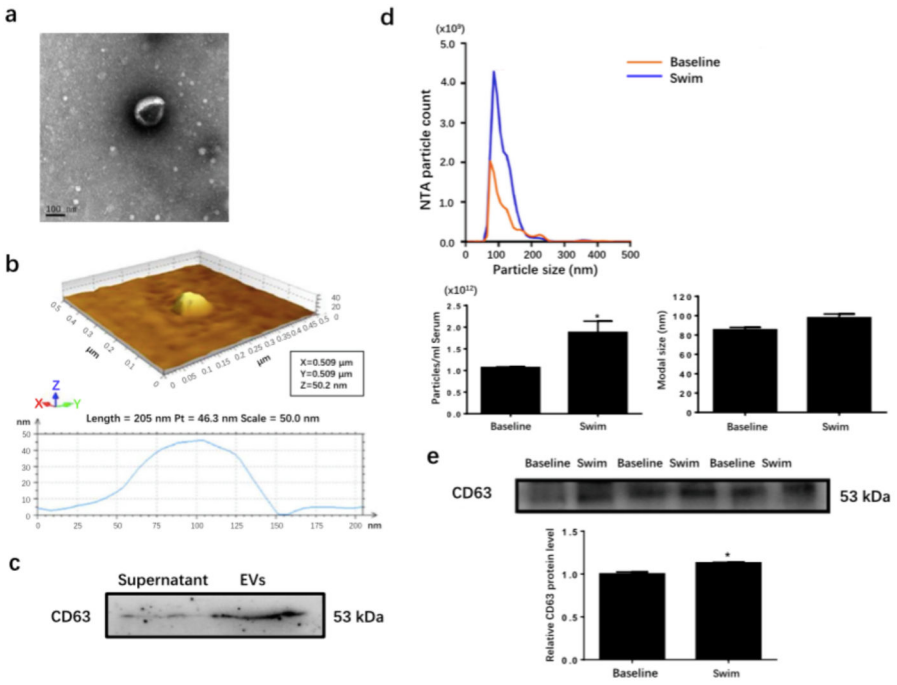

Figure 2. Increased serum extracellular vesicle level in response to chronic exercise

(a and b) Transmission electron microscopy and atomic force microscopy for EVs isolated from the serum. Scale bar=100 nm. **(c)** Western blot for exosomal marker CD63 (n=3). **(d)** Nanoparticle tracking analysis for average concentration and modal size of EVs in the serum (n=4). **(e)** Western blot showed increased CD63 expression level in EVs extracted from the serum of swum mice (n=3). EVs, extracellular vesicles. *, $P<0.05$.

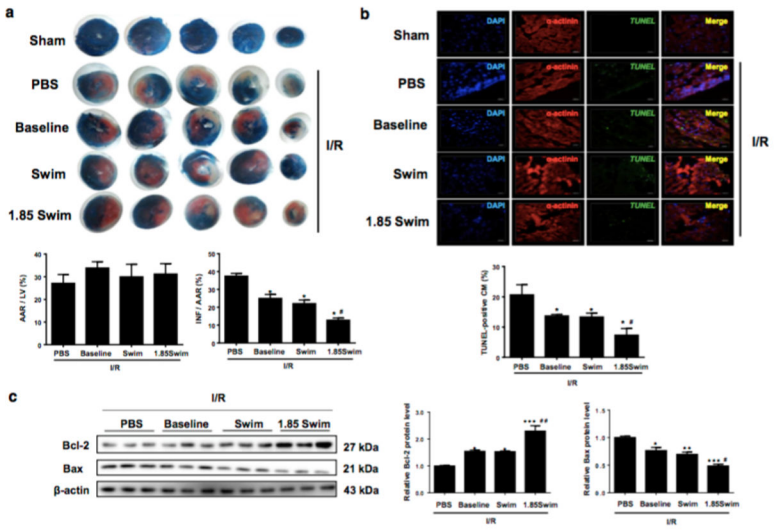

Figure 3. Exercise-induced increase in serum extracellular vesicles reduces cardiac ischemia/ reperfusion (I/R) injury

(a) Heart samples were stained with 2,3,5-triphenyltetrazolium chloride (TTC) to examine the infarct size after I/R injury (n=6). **(b)** TUNEL-positive nuclei in α-actinin-labeled cells were calculated to determine myocardial apoptosis (n=6). Scale bar=20 μm. **(c)** Western blot for Bcl-2 and Bax in heart samples (n=3). AAR, area at risk; INF, infarct size; LV, left ventricle; CM, cardiomyocytes. *, $P<0.05$ *vs.* PBS group; #, $P<0.05$ *vs.* Swim group.

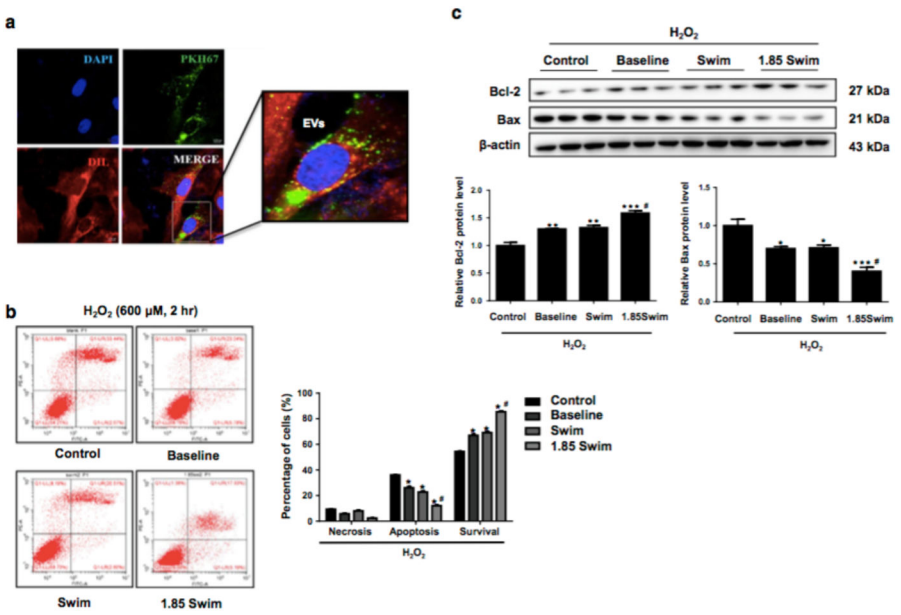

Figure 4. Exercise-derived circulating extracellular vesicles provide anti-apoptotic effect in cardiomyocytes

(a) Representative image of PKH67 labeling (green) to verify the uptake of EVs by H9C2 cells after 24 hours of incubation. Dil dye (red) was added for cell membrane staining. Nuclei were couterstained with DAPI (blue). Scale bar=20 μm. **(b and c)** Flow cytometry analysis for apoptosis (n=5) and Western blot for Bcl-2 and Bax (n=3) in H_2O_2-treated H9C2 cells with pre-incubation of EVs or controls. EVs, extracellular vesicles. *, $P<0.05$ *vs.* Control group; #, $P<0.05$ *vs.* Swim group.

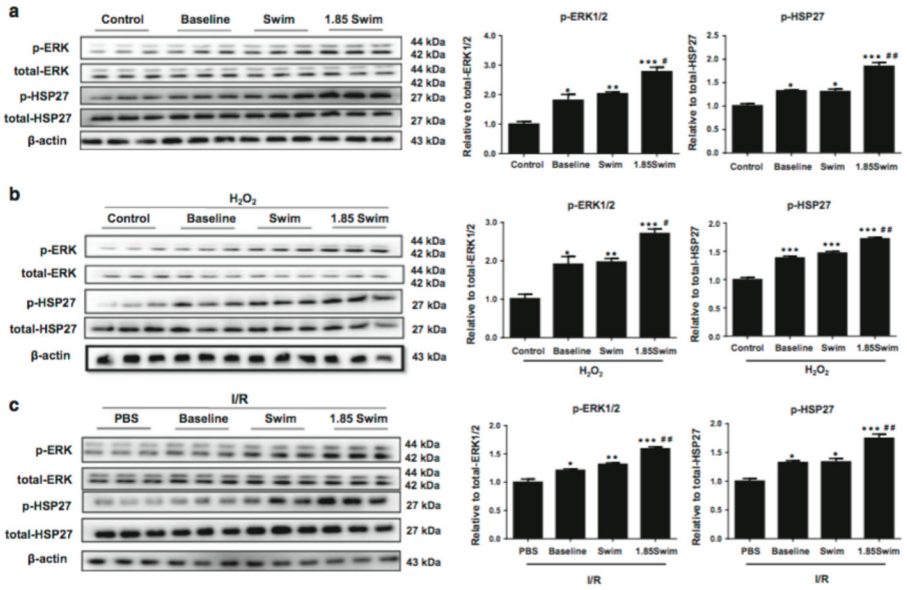

Figure 5. Activation of ERK1/2 and HSP27 by exercise-derived extracellular vesicles

(a) Western blot for ERK1/2 and HSP27 phosphorylation level in H9C2 cells pretreated with EVs or controls (n=3). **(b)** Western blot for ERK1/2 and HSP27 phosphorylation level in H_2O_2-treated H9C2 cells with pre-incubation of EVs or controls (n=3). **(c)** Western blot for ERK1/2 and HSP27 phosphorylation level in I/R hearts pretreated with EVs or PBS (n=3). EVs, extracellular vesicles. *, $P<0.05$ *vs.* Control or PBS group; #, $P<0.05$ *vs.* Swim group.

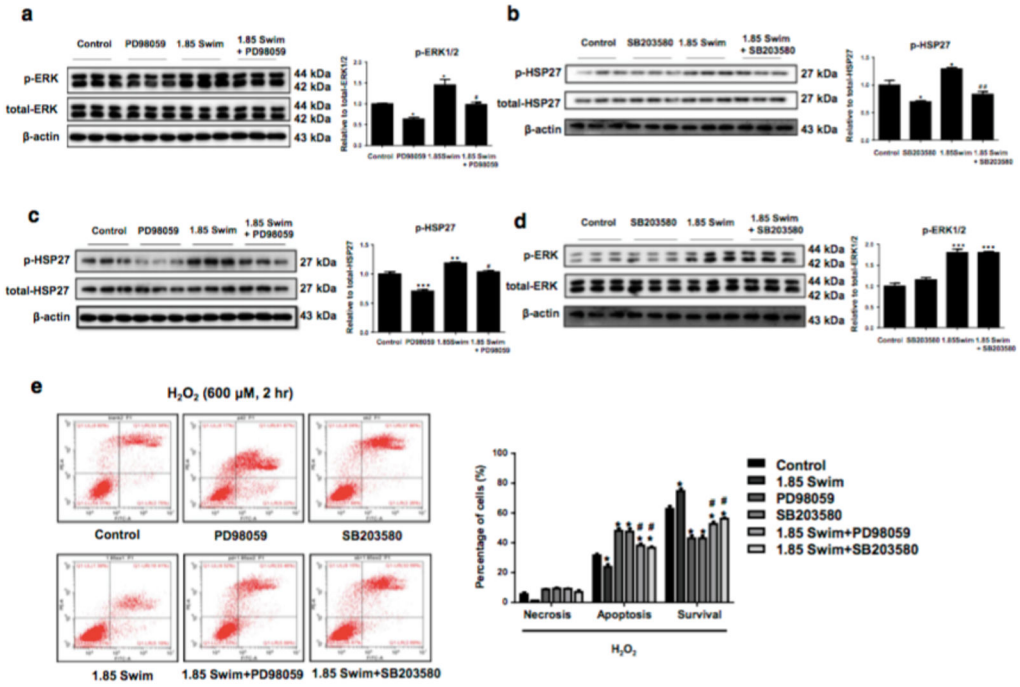

Figure 6. Activation of ERK1/2 and HSP27 is essential for the anti-apoptotic effect of exercise-derived extracellular vesicles in cardiomyocytes

(a and c) Inhibition of ERK1/2 via PD98059 reduced ERK1/2 and HSP27 phosphorylation level in H9C2 cells (n=3). **(b and d)** Inhibition of HSP27 via SB203580 reduced HSP27 but not ERK1/2 phosphorylation level, confirming HSP27 as a downstream effector of ERK1/2 (n=3). **(e)** Flow cytometry showed that inhibition of ERK1/2 or HSP27 abolished the anti-apoptotic effect of exercise-induced increase of EVs in H_2O_2-treated H9C2 cells (n=5). EVs, extracellular vesicles. *, $P<0.05$ *vs.* Control group; #, $P<0.05$ *vs.* 1.85 Swim group.

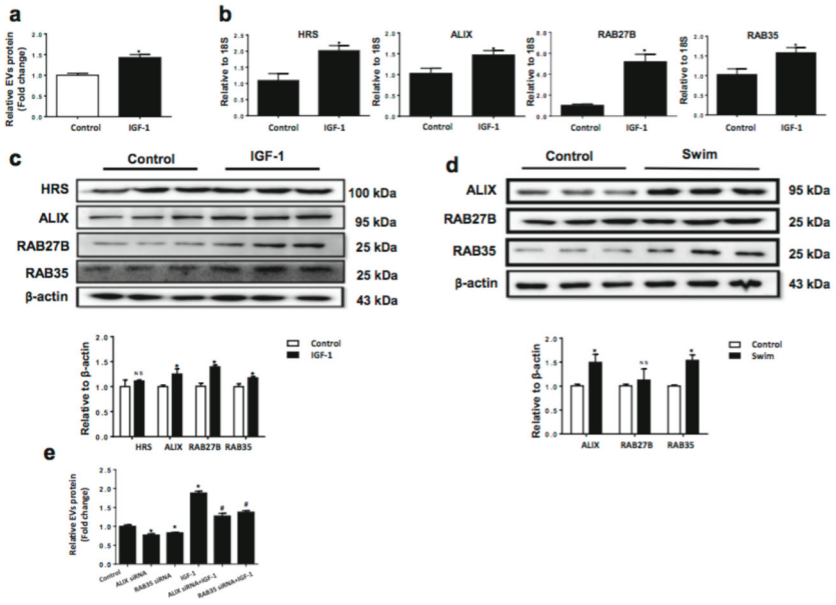

Figure 7. IGF-1 via activating ALIX and RAB35 induces extracellular vesicles release from cardiomyocytes

(a) IGF-1-treated H9C2 cells have increased release of EVs (n=3). **(b)** qRT-PCR for HRS, ALIX, RAB27B, and RAB35 mRNA levels in IGF-1-treated H9C2 cells (n=6). **(c and d)** Western blot showed that ALIX and RAB35 protein levels were increased in IGF-1-treated H9C2 cells (n=3) and heart samples from swum mice (n=3). **(e)** Knockdown of ALIX or RAB35 via siRNA reduced IGF-1-induced release of EVs from H9C2 cells (n=4). EVs, extracellular vesicles. *, $P<0.05$ *vs.* Control group; #, $P<0.05$ *vs.* IGF-1 group.

Table 1

Primer sequences for qRT-PCRs

Gene	Species	Forward primer (5′-3′)	Reverse primer (5′-3′)
ALIX	Rat	GCAGAGCAGAACCUGGAUATT	UAUCCAGGUUCUGCUCUGCTT
HRS	Rat	TGAGTGGCTGTCGAGTGTTC	TCGTGACCTGCTTCTTGACC
STAM1	Rat	ACATCAAGGCATGGGGCTTT	TGGTGACACATCGCTTCGAG
TSG101	Rat	ATCCTGGCTGTCCTTACCCA	TGCTCGAATAGTGTCCTCGC
RAB11	Rat	ATTCAGGTGGACGGCAAGAC	CACCACGGTAGTACGCAGAG
RAB27A	Rat	GTTCGACCTGACAAACGAGC	CTTTCACAGCCCTCTGGTCT
RAB27B	Rat	CCGAUACACAGACAAUAAATT	CCAUGGGCUUCUUACUAAUTT
RAB35	Rat	GCAGCUACAUCACCACAAUTT	AUUGUGGUGAUGUAGCUGCTT
18s	Rat	ATTCGAACGTCTGCCCTATCAA	CGGGAGTGGGTAATTTGCG